Proceedings of the 9th World Congress on Civil, Structural, and Environmental Engineering (CSEE 2024)
London, United Kingdom – April 14-16, 2024
Paper No. ICGRE 136
DOI: 10.11159/icgre24.136

Seismic Fragility Functions of a Tailings Dam Affected by Subduction Earthquakes

Nestor Bellido[1], Zenón Aguilar[1]
[1]National University of Engineering
Civil Engineering Faculty, Lima, Peru
First.nbellidoa@uni.pe; Second.zaguilar@uni.edu.pe

Abstract **-** The seismic response of tailings dams is highly dependent on the intensity measures (IMs) of the input ground motions. For this reason, several researchers have used seismic fragility functions to evaluate the seismic performance of geotechnical structures. Seismic stability analyses of tailings dams are further challenged by the uncertainty and variability of IMs for a given earthquake scenario and site conditions. This study presents the seismic performance of a tailings dam affected by subduction earthquakes by generating fragility functions and analysing the effectiveness of different IMs in predicting a damage measure (DM), such as horizontal displacements. Our analyses are based on finite-difference numerical simulations using advanced constitutive models. The selected ground motions are compatible with the Maximum Credible Earthquake (MCE), which is common in the practice in South America. The results show that the Arias intensity is the most efficient and optimal IM in predicting the horizontal crest displacements of the dam. Furthermore, the analytical fragility functions based on numerical results using peak ground acceleration (PGA), Arias intensity (AI), cumulative absolute velocity (CAV), and peak ground velocity (PGV) are presented. The fragility functions can be a useful tool to assess the probability of damage levels for designed tailings dams based on their design earthquake and acceptable risk. In addition, the obtained fragility functions could be used to define alert levels to be considered in the operation manual of the tailings storage facility (TSF).

Keywords**:** Fragility functions, tailings dam, subduction earthquakes, dynamic analyses, efficiency

1. Introduction

The design of tailings dams involves the necessity to perform nonlinear dynamic analyses (NDAs) to verify the seismic stability of the dams, especially in areas of high seismicity such as the South American Andes, which are part of the Pacific Ring of Fire. On a large scale, the tectonic framework is determined by the interaction between the Nazca and South American plates. In the current state of practice for seismic evaluation of slope displacements in subduction tectonic settings, several procedures are available (e.g., [1,2]). These available procedures can be used to estimate permanent displacements in tailings dams, with certain limitations. However, when potentially liquefiable materials affect the seismic performance of structures, more rigorous procedures, such as nonlinear dynamic analyses, should be employed.

Fragility curves are one of the key elements of probabilistic seismic risk assessment of the built environment and lifeline system [3]. They relate the IMs to the probability of reaching or exceeding a damage state (e.g., minor, moderate, major, severe, collapse) for each element at risk. Given the diversity of ground motion IMs, several researchers have evaluated their effectiveness, predictability, and total uncertainty. Recently, studies have been conducted on the uncertainty analysis of different IMs in predicting damage levels. Regina et al. [4], found that the CAV is the optimal IM in predicting the vulnerability of earth dams and the fragility functions based on the CAV have the lowest standard deviation values. Armstrong et al. [5], found that the AI was the most efficient IM, however, the CAV has the lower total standard deviation in the evaluation of earth dams. Boada et al. [6] propose fragility curves for abandoned tailings dams in Chile as a function of the spectral acceleration at a vibration period of 0.3s, Sa(0.3s), this IM shows a lower efficiency but was finally selected due to its high predictability when compared to the more efficient alternatives.

The purpose of this study is to present fragility functions and efficiency analyses of IMs to assess the probability of damage levels for a tailings dam based on horizontal crest displacements. Furthermore, according to the results, it would be possible to define alert levels to be considered in the operation manual of the tailings storage facility (TSF) and design criteria.

2. Numerical modelling

The tailings dam geometry considered in this study is representative of an existing Peruvian tailings dam constructed using the downstream method (referent to rockfill). The numerical modelling is performed using the commercial 2D finite difference software platform FLAC [7], which is based on an explicit time-marching method to solve the equations of motion. The zone sizes in FLAC are chosen to ensure accurate high frequencies wave transmission based on the recommendations of Kuhlemeyer and Lysmer [8]. Ground motion frequencies greater than 15 Hz were filtered out, as they carry a relatively small amount of energy, as described by Mánica et al [9]. The size of the FLAC zones was 1.0 m in both vertical and horizontal directions. In the model, the boundaries were sufficiently far from the failure zone to minimize the influence of the boundaries on the model response. A free field boundary condition was applied to the side boundaries and a quiet boundary was considered at the bottom boundary in both the horizontal and vertical directions during the dynamic analyses. The outcrop input motions were applied in a form of shear stress at the base of the model using the compliant-base procedure of Mejia and Dawson [10]. A Rayleigh damping of 0.5% at a center frequency of 2.5 Hz was used during the dynamic loading. The tailings were assumed to be saturated and liquefiable; therefore, the fourth columns of the zones at the far left boundary was assumed to be non-liquefiable to avoid inaccurate free field boundary calculations, as recommended by Boulanger and Ziotopoulou [11]. The initial stress state for the tailings dam is estimated using a five-state procedure. Seepage analyses are performed with an uncoupled fluid flow calculation, groundwater boundary conditions were applied to the model to obtain a water table that descends through the filter/drain location and to ensure a saturated condition for the tailings. Three different constitutive models are used in this study. For the materials susceptible to liquefaction (tailings), the PM4Silt V2.1 model [11] is used. The behaviour of the foundation bedrock is assumed to be linear elastic, while all the other materials are characterized by the UBCHyst model [12]. PM4Silt is a plane strain-stress ratio-controlled, critical state-compatible, bounding surface plasticity model for clays and plastic silts and has recently been used to represent tailings (e.g., [13,14,15]). Calibration of this model is performed with single-element simulations for the range of loading paths important for the tailings. In this study, the PM4Silt parameters are calibrated to obtain a cyclic resistance to liquefaction curve that matches that estimated from cyclic direct simple shear (CDSS) tests. UBCHyst is a robust, relatively simple, total stress model. It uses the Mohr-Coulomb failure criterion, extended with a formulation for shear secant modulus reduction with strain. The UBCHyst parameters of the rockfill and filter/drain material are calibrated to be consistent with the G/G_{max} ratio and damping curves of Rollins et al. [16] and Darendeli [17], respectively. The filter/drain material is located between the rockfill-tailings and rockfill-bedrock interfaces.

Figure 1 shows the dam geometry model generated in FLAC. The bedrock has a length of 1100 m and a thickness of 50 m, the tailings have a height of 100 m, and the rockfill has a height of 101 m with a crest length of 10 m. The downstream slope is a 2.0H:1.0V and the upstream slope is 1.5H:1.0V.

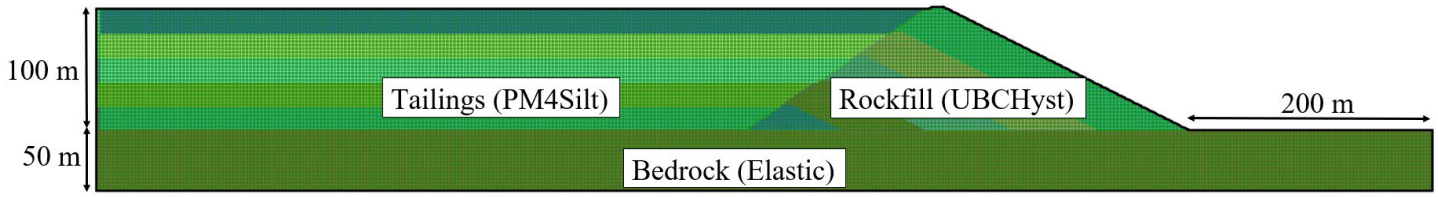

Fig. 1: Meshes of the analysed tailings dam.

The rockfill strength parameters for the dynamic analyses were estimated based on average data from Leps [18]. The friction angle ϕ' was estimated based on Barton and Kjaersnli [19], using equation 1.

$$\phi = \phi_1 - \Delta\phi log\left(\frac{\sigma'_3}{Pa}\right) \quad (1)$$

where σ'_3, $\phi 1$, $\Delta\phi$ and Pa are minor principal effective stress, reference friction angle (at $\sigma'_3=Pa$), friction angle reduction for each log cycle of stress level increase, and atmospheric pressure (101.3 kPa), respectively.

In the case of the filter/drain and rockfill, G_{max} was estimated using the equation 2 proposed by Seed et al. [20]. The bedrock was simulated as an elastic material with a stiffness corresponding to shear wave velocity of 760 m/s and the stiffness properties of the tailings were obtained from the resonant column and torsional shear (RCTS) test calibrated with the parameters considered for the PM4Silt model.

$$G_{max} = 21.7 k_{2,max} Pa \left(\frac{p'}{Pa}\right)^{0.5} \quad (2)$$

where G_{max}, $k_{2,max}$, and p' are the small strain shear modulus, modulus coefficient, and the mean effective pressure, respectively.

The summary of the strength parameters, UBCHyst, and PM4Silt parameters for a tailings dam is shown in Table 1. Tailings parameters are shown in Table 1 (the secondary parameters for the PM4Silt model not shown in the table were kept at the default value) divided by an effective vertical stress (σ'_{vc}) of 400 kPa (according to laboratory test). Tailings 1, $\sigma'_{vc} \leq$ 400 kPa and Tailings 2, $\sigma'_{vc} >$ 400 kPa.

Table 1: Parameters adopted for the tailings dam.

Input parameters	Property	Rockfill	Filter/drain	Tailings 1 / 2	Bedrock
Dry unit weight	γ_{dry} (kN/m^3)	22	16	16.3 / 17.5	25
Cohesion	c'	-	0	-	-
Friction angle	ϕ'	$\phi 1$=45.5 $\Delta\phi$=6.55	35	-	-
Small strain shear modulus	G_{max} (MPa)	-	-	-	1500
Modulus coefficient	$k_{2,max}$	180	110	-	-
Poisson ratio	υ	0.30	0.33	-	0.25
PM4Silt					
Undrained shear strength ratio at critical state	$S_{u,cs}/\sigma'_{vc}$	-	-	0.15 / 0.15	-
Shear modulus coefficient	G_o	-	-	602 / 602	-
Contraction rate parameter	h_{po}	-	-	5.5 / 10	-
Initial void ratio	e_o	-	-	0.8 / 0.66	-
Shear modulus exponent	n_G	-	-	0.7 / 0.7	-
Critical state friction angle	ϕ'_{cv}	-	-	31 / 31	-
Compressibility in e-ln(p') space	λ	-	-	0.06 / 0.06	-
UBCHyst					
UBCHyst calibration parameters	H_n	1	1	-	-
	H_{rf}	0.7	0.98	-	-
	H_{rm}	1	1	-	-
	H_{dfac}	0.8	0.6	-	-
	H_{dmodfl}	2	1	-	-

Figure 2 shows the derived PM4Silt based cyclic resistance curves calibration against laboratory cyclic direct simple shear (CDSS) for a cyclic strain of 3.75%. Figure 3 shows the ability of the PM4Silt model to capture the undrained cyclic behaviour of the tailings, successfully capturing the key cyclic behaviour in terms of cyclic strain accumulation and pore pressure generation.

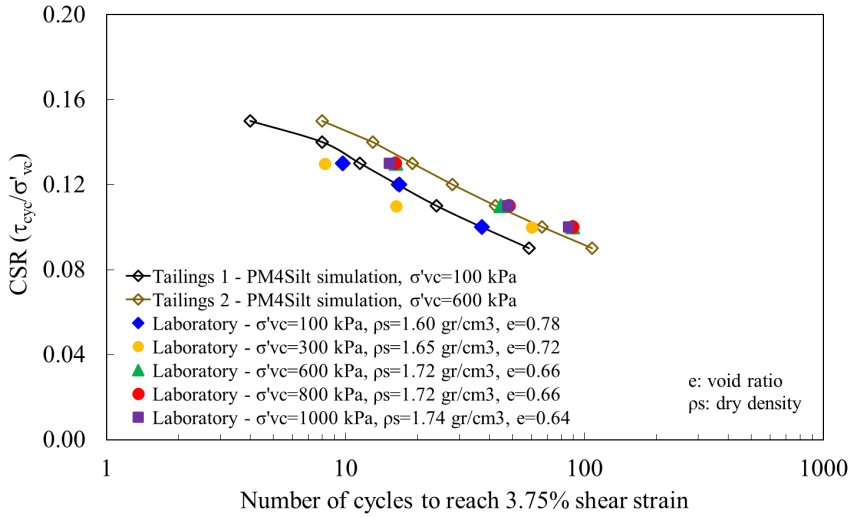

Fig. 2: Cyclic stress ratio (CSR) plotted against number of cycles needed to reach 3.75% shear strain in undrained cyclic simple shear (CSS) tests for tailings 1 and tailings 2.

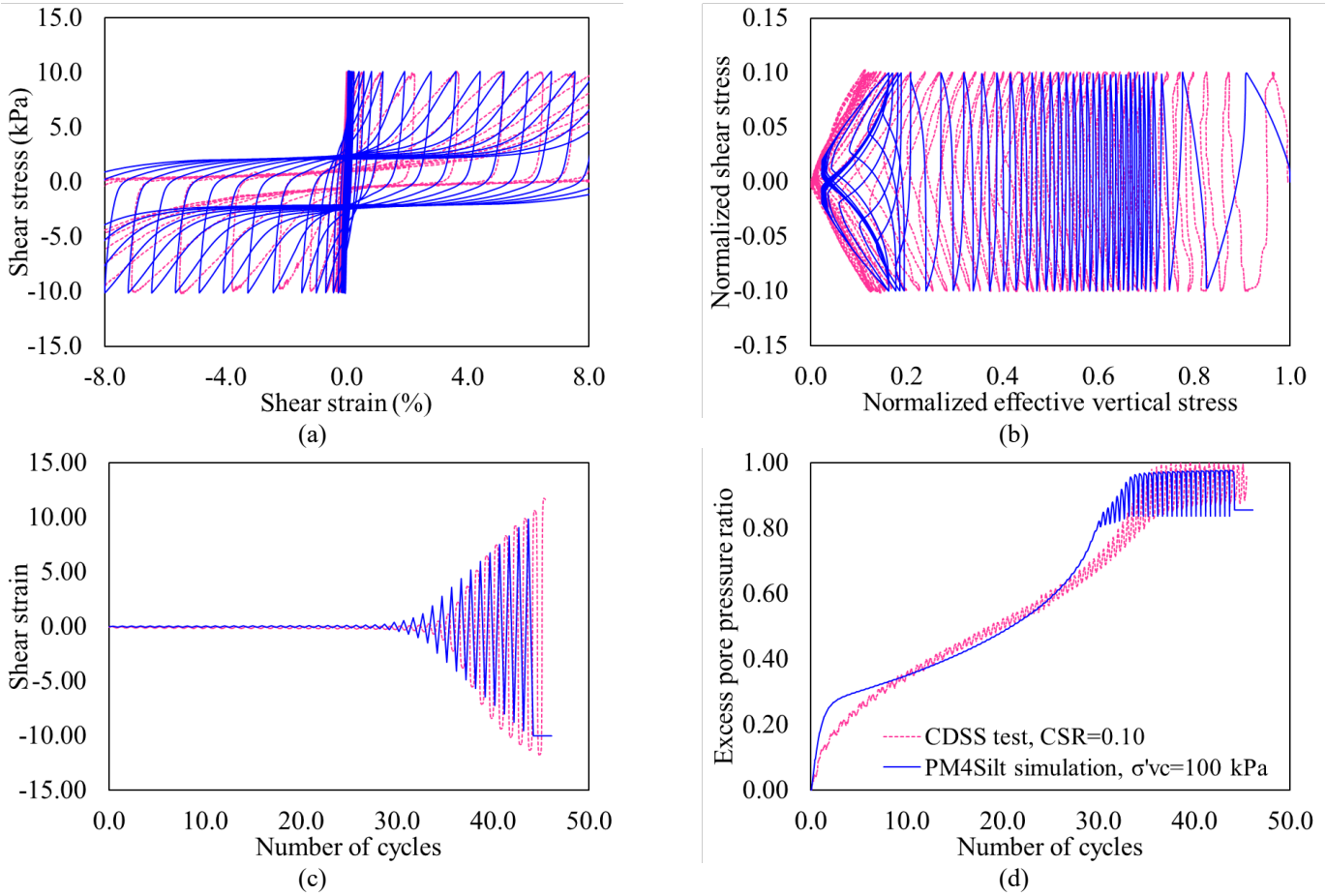

Fig. 3: Comparison of calibrated and experimental response of mine tailings 1, considering CSS test with CSR=0.10 and confinement of 100 kPa.

Figure 4 shows a comparison of the G/G_{max} and damping ratio curves calibrated in FLAC for the rockfill.

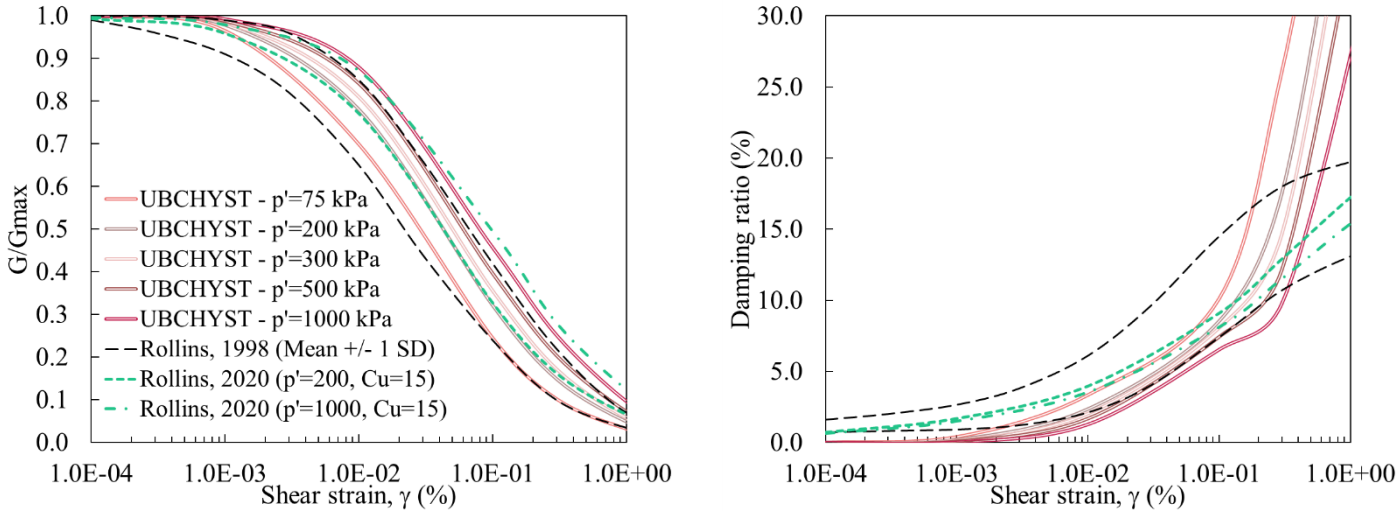

(a) (b)

Fig. 4: UBCHYST model calibration for the rockfill (Cu: uniformity coefficient; SD: standard deviation).

Furthermore, a sensitivity assessment of the results was conducted, considering a bedrock thickness of 100 m in the FLAC model. For this purpose, three records obtained through the spectral matching method (detailed in a subsequent section) were employed. The analysis revealed a decrease in horizontal crest displacements in the range of 4 to 6 %. Nevertheless, it is strongly recommended to assess the influence of bedrock thickness on the response of tailings dams to ensure that results are not influenced by boundary conditions.

3. Input ground motions

Two methods were considered for the selection of ground motions. The first one, described by Baker and Lee [21], for which candidate ground motions were selected from different institutions such as CISMID, CSN, IGP, COSMOS, and RENADIC. The generated database contains more than 251 ground motions, mainly from subduction interface and intraslab earthquakes recorded in Chile and Peru. According to this methodology, a total of 15 ground motions (with an average shear wave velocity in the upper 30 m between 600 m/s$\leq V_{s30} \leq$950 m/s) were selected, that were compatible with the Maximum Credible Earthquake (MCE) and its associated standard deviation obtained from the deterministic seismic hazard analysis (DSHA) for soil type BC, V_{s30}=760 m/s. The second method involves the generation of synthetic ground motions using the spectral matching method (described by Al Atik and Abrahamson [22]), 7 ground motions were considered with a target spectrum obtained from the 84th percentile MCE, these ground motions correspond to intraslab earthquakes.

The first method was considered to include ground motions with different intensity measures that are collectively compatible with a target spectrum and its associated standard deviation. Meanwhile, the second method, which is commonly used in current engineering practice, provides ground motions that are compatible with a target spectrum without having variability in the response spectra; however, they have different intensity measures. Figure 5 shows the response spectra of the 22 selected ground motions compared to the response spectra of the MCE with different percentiles.

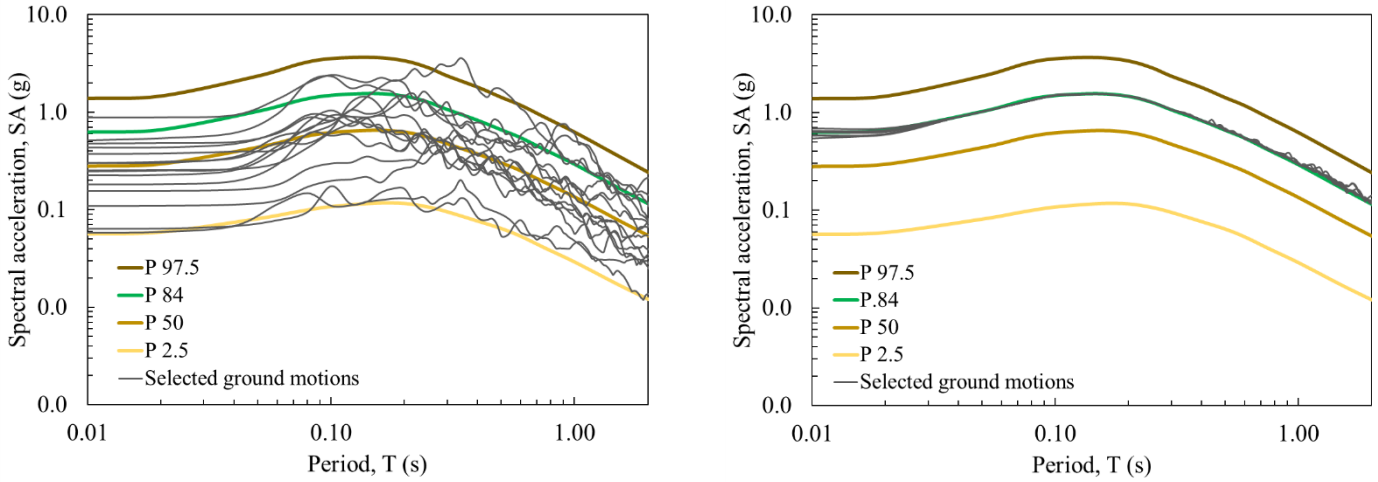

Fig. 5: Response spectra of the selected ground motions using (a) the methodology developed by [21] and (b) the spectral matching method described by [22].

4. Evaluation of optimal ground motion intensity measures

According to Regina et al. [4], the correlation between an intensity measure (IM) and the target damage measure (DM) can be synthesized by a single property of the selected IM: its efficiency (i.e., how well the IM is correlates with a given DM). The estimated IMs of the input ground motions for this study were peak ground acceleration PGA, peak ground velocity PGV, Arias intensity AI, and spectral accelerations SA. Rathje and He [23], described that the median of the structural demand in terms of IM (note that S_D is the model prediction of DM), can be expressed as:

$$\ln\big(S_D(\mathrm{IM})\big) = \ln(a) + b.\ln(IM) \tag{3}$$

It is also assumed that the DM model follows a lognormal distribution. Thus, the distribution of the logarithm of the data (e.g., ln(DM)) at a given IM follows a normal distribution with a mean given by equation (3) and a standard deviation of $\sigma_{\mathrm{lnDM|lnIM}}$. This standard deviation of the regression model in equation (3), using the predicted and the measured values, is given by:

$$\sigma_{\mathrm{lnDM|lnIM}} = \sqrt{\frac{\sum_i^N [\ln(\mathrm{DM_i}) - \ln(S_D(\mathrm{IM_i}))]^2}{N-2}} \tag{4}$$

where $\mathrm{DM_i}$ is the recorded maximum value of the demand parameter from each analysis and N is the number of analyses performed.

In the present study, we considered the horizontal crest displacement as a DM. However, different DMs could be considered, such as: filter displacement, free board reduction, normalized crest settlement and even the excess pore water pressure (r_u) for materials that pose a risk to the seismic stability of TSFs. Figure 6 shows the horizontal crest displacements with some intensity measures (PGA, AI, CAV, and PVG) of the input ground motions. The green circles show the input ground motions from the methodology developed by Baker and Lee [21], and the blue circles show those obtained by the spectral matching methodology.

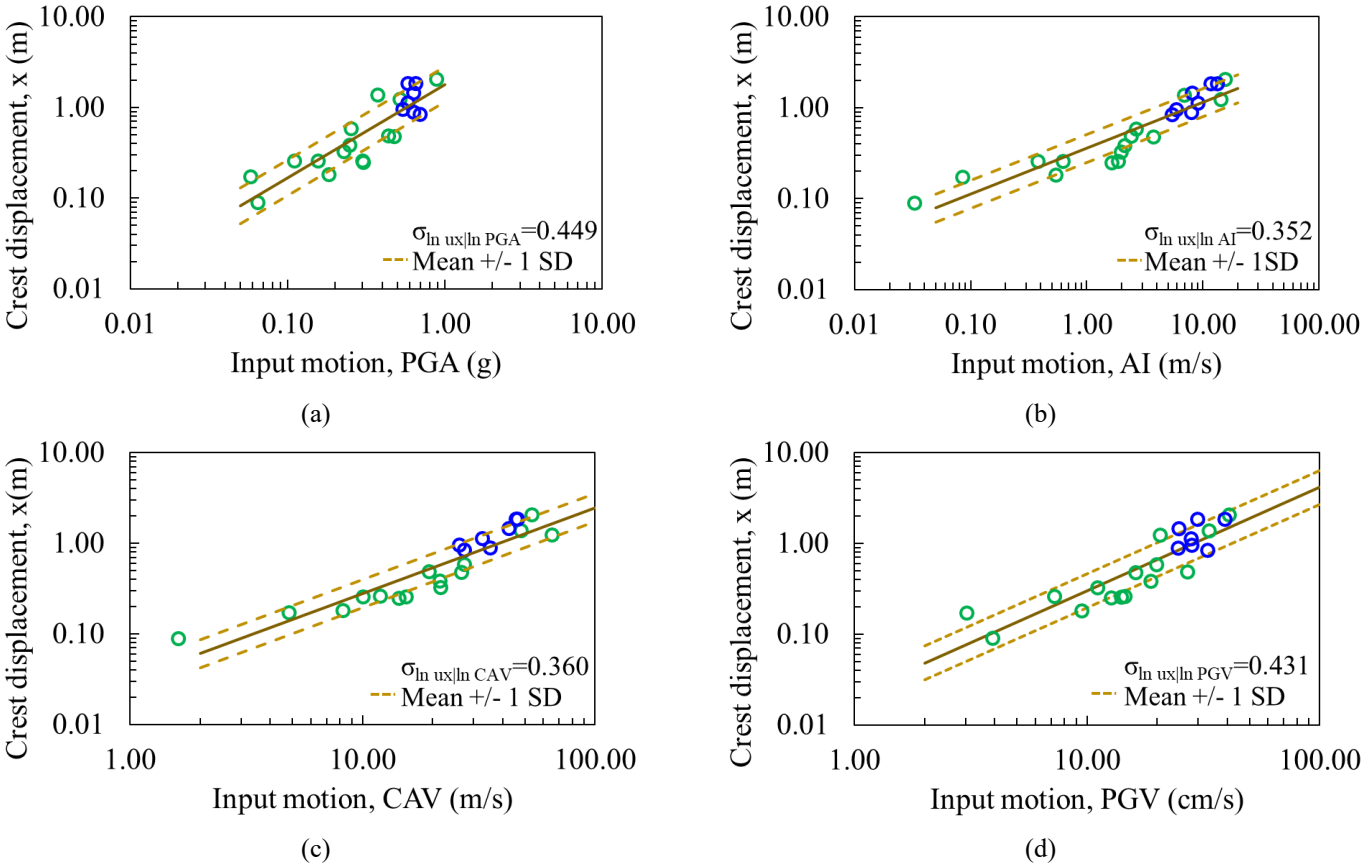

Fig. 6: Ground motion IM efficiency of the horizontal crest displacements of a tailings dam: (a) PGA, (b) AI, (c) CAV, and (d) PGV.

Figure 7 shows the standard deviations of the horizontal crest displacements for different intensity measures. The standard deviation of the spectral acceleration is presented for a period of 0.4 seconds, because it is consistent with the fundamental period of the tailings dam (undamped analysis estimate).

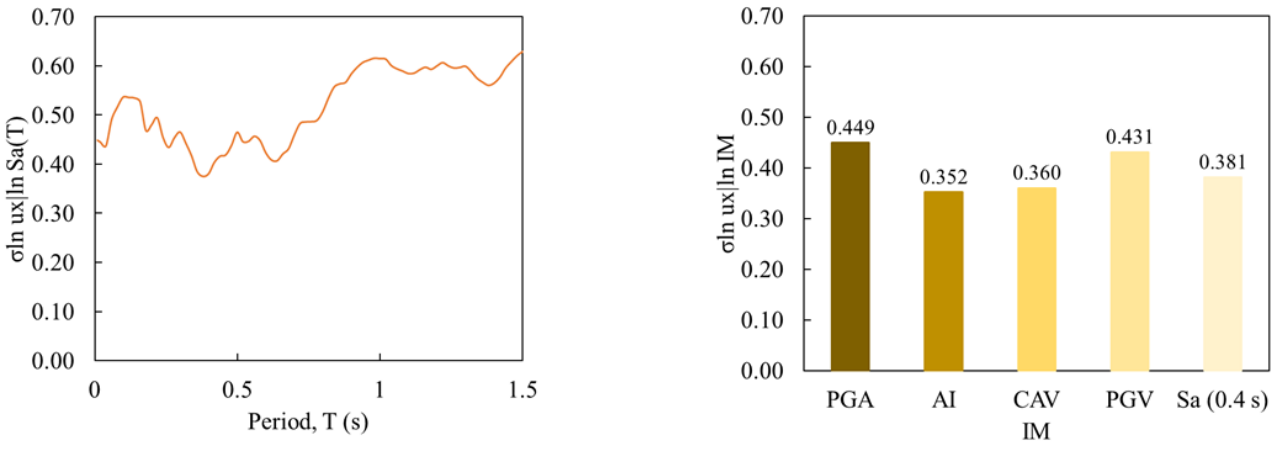

Fig. 7: (a) Dispersion of the horizontal crest displacement ux conditioned to spectral acceleration with 5% damping ratio at different periods Sa(T). (b) Summary of dispersion indices for different IMs.

Analysis of IM predictability is incorporated as suggested by Armstrong et al. [5] by calculating the total standard deviation as:

$$\sigma_{\mathrm{lnDM|M,R,S}} = \sqrt{\sigma^2_{lnDM|lnIM} + b^2.\sigma^2_{lnIM|M,R,S}} \tag{5}$$

where $\sigma_{\mathrm{lnIM}|M,R,S}$ is the standard deviation of a ground motion model (GMM), representing its predictability, and b is the slope of the least-square linear regression on a log-log scale.

However, for the present evaluation, the standard deviations representing the predictability, $\sigma_{\mathrm{lnIMsec|lnIMp}}$, were estimated by the conditional ground motion models (CGMMs), according to the 84th percentile MCE, for different IMs such as AI, CAV, and PGV developed by Macedo et al [24], Liu and Macedo [25,26], respectively. These CGMMs were developed for subduction earthquakes. Finally, the analysis of the optimal IM considering CGMMs is as follows:

$$\sigma_{\mathrm{lnDM|lnIMp}} = \sqrt{\sigma^2_{lnDM|lnIMsec} + b^2.\sigma^2_{lnIMsec|lnIMp}} \tag{6}$$

where IM_{sec} represents a secondary IM and IM_p represents the observed primary IM, as described by Macedo et al. [27]. Table 2 shows the efficiency, predictability, and total standard deviation for AI, CAV, and PGV.

Table 2: Efficiency, predictability, and total standard deviation for tailings dam, horizontal crest displacements, for AI, CAV, and PGV for CGMMs.

IM	Efficiency $\sigma_{\mathrm{lnDM|lnIMsec}}$	Predictability $\sigma_{\mathrm{lnIMsec|lnIMp}}$	Total standard deviation $\sigma_{\mathrm{lnDM|lnIMp}}$	Value of mean IM according CGMMs
AI	0.352	0.331	0.389	7.59 m/s
CAV	0.360	0.302	0.459	31.57 m/s
PGV	0.431	0.374	0.603	24.23 cm/s

5. Fragility functions for different IMs

The seismic performance of tailings dams can be evaluated using fragility functions, which provide the probability of structures reaching (or exceeding) a given limit state (or damage measure, DM) for each level of ground motion intensity measure (IM). It can be expressed as:

$$P(d > \mathrm{DM}|\mathrm{IM} = x) \tag{7}$$

In this study, analytical fragility functions are considered because they are based on the results of numerical models. A lognormal cumulative distribution function (CDF) is often used to define a fragility function [3].

$$P(d > \mathrm{DM}|\mathrm{IM} = x) = \Phi\left(\frac{\ln\frac{x}{\theta}}{\beta}\right) \tag{8}$$

where Φ is the standard normal CDF, x is the IM, θ is the IM corresponding to 50% exceedance probability (i.e., the median), and β is the total natural log standard deviation.

The development of the fragility curves according to equation 8 requires the estimation of θ and β from the results of dynamic analyses. Following the approach of HAZUS [28], the uncertainty associated with the definition of the damage

measure states (β_{DS}) is set equal to 0.4. The uncertainty associated with the capacity (β_C) is set equal to 0.25. The last source of uncertainty, related to the seismic demand, is described by the variability of the response due to the variability of the ground motions ($\beta_D = \sigma_{\ln DM|\ln IM}$, efficiency).

$$\beta = \sqrt{\beta_{DS}^2 + \beta_C^2 + \beta_D^2} \tag{9}$$

Baker [29] presents various methods for computing fragility functions for structural systems (e.g., incremental dynamic analysis, IDA; multiple stripe analysis, MSA), which have recently been used by different researchers (e.g., [4,6]) to evaluate dams because they use a significant number of earthquakes. However, in the present evaluation, the 22 earthquakes described above, which are compatible with the MCE spectrum, were considered for the construction of fragility curves according to the procedure of Argyroudis et al. [3]. Figure 8 shows the fragility functions for the horizontal crest displacements as DM with some values of the limiting displacement (i.e., 1.00, 0.50, 0.25, and 0.15 m).

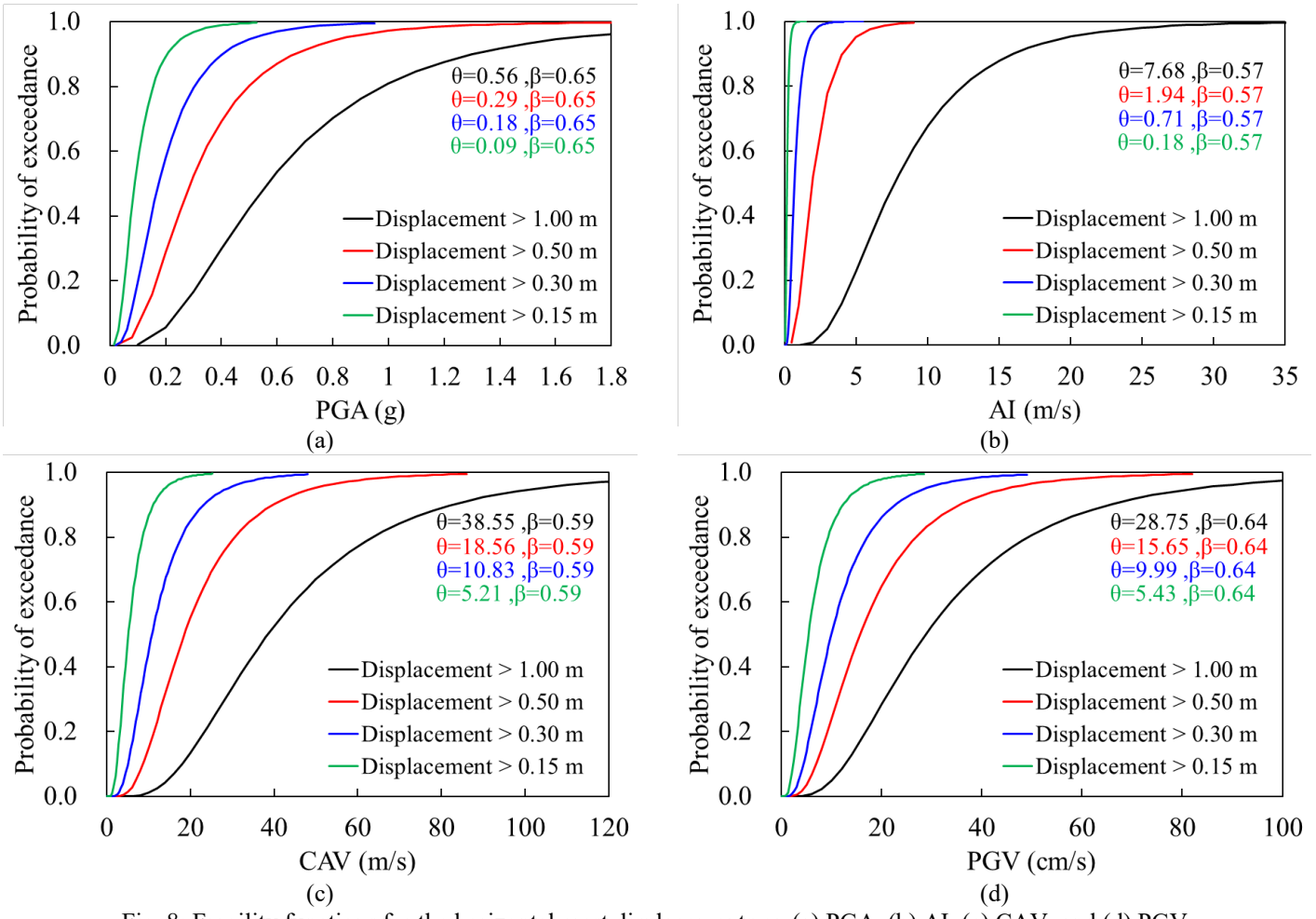

Fig. 8: Fragility functions for the horizontal crest displacements on (a) PGA, (b) AI, (c) CAV, and (d) PGV.

6. Conclusion

This study presents the seismic performance of a tailings dam in central Peru, located in an area of high seismicity. The geotechnical characterization was used to provide inputs to the PM4Silt model, which was used to represent the cyclic response of the tailings and the UBCHyst model was used for the rockfill and filter/drain, as they are not expected to generate pore pressure under cyclic loading.

The correlation between IMs and DM (horizontal displacements) for the tailings dam indicated that the most efficient and optimal IM was the AI in predicting the horizontal crest displacements and it is found that the spectral acceleration at a period of 0.4s (fundamental period of the tailings dam), Sa (0.4s), shows a high efficiency than other spectral accelerations.

The available fragility functions for the tailings dam vulnerability assessment could be used to define alert levels under seismic loading with a certain level of risk that is acceptable for a tailings dam. CGMMs are developed to estimate IMs (e.g., AI, CAV, PGV) for earthquakes in subduction zones that have a lower total standard deviation than those estimated by traditional GMMs. These estimated IMs are consistent with a given spectral acceleration of the design response spectrum (e.g., 84th percentile MCE). The IMs estimated by CGMMs, along with the fragility curves, can be used to define a range of exceedance probability of the design DM.

Acknowledgements

The authors would like to acknowledge the support of Carlos Sánchez for processing the information employed in this study.

References

[1] J. D. Bray, J. Macedo, and T. Travasarou, "Simplified Procedure for Estimating Seismic Slope Displacements for Subduction Zone Earthquakes," *Journal of Geotechnical and Geoenvironmental Engineering*, vol. 144, no. 3, Mar. 2018, doi: 10.1061/(ASCE)GT.1943-5606.0001833.

[2] J. Macedo, J. D. Bray, and C. Liu, "Seismic Slope Displacement Procedure for Interface and Intraslab Subduction Zone Earthquakes," *Journal of Geotechnical and Geoenvironmental Engineering*, vol. 149, no. 11, Nov. 2023, doi: 10.1061/JGGEFK.GTENG-11445.

[3] S. Argyroudis, A. M. Kaynia, and K. Pitilakis, "Development of fragility functions for geotechnical constructions: Application to cantilever retaining walls," *Soil Dynamics and Earthquake Engineering*, vol. 50, pp. 106–116, Jul. 2013, doi: 10.1016/j.soildyn.2013.02.014.

[4] G. Regina, P. Zimmaro, K. Ziotopoulou, and R. Cairo, "Evaluation of the optimal ground motion intensity measure in the prediction of the seismic vulnerability of earth dams," *Earthquake Spectra*, vol. 39, no. 4, pp. 2352–2378, Nov. 2023, doi: 10.1177/87552930231170894.

[5] R. Armstrong, T. Kishida, and D. Park, "Efficiency of ground motion intensity measures with earthquake-induced earth dam deformations," *Earthquake Spectra*, vol. 37, no. 1, pp. 5–25, Feb. 2021, doi: 10.1177/8755293020938811.

[6] G. Boada, C. Pasten, and P. Heresi, "Analytical fragility curves for abandoned tailings dams in North-Central Chile," *Soil Dynamics and Earthquake Engineering*, vol. 164, p. 107637, Jan. 2023, doi: 10.1016/j.soildyn.2022.107637.

[7] Inc. (2019) Itasca Consulting Group, "FLAC — Fast Lagrangian Analysis of Continua, Ver. 8.1." Minneapolis: Itasca.

[8] R. L. Kuhlemeyer and J. Lysmer, "Finite Element Method Accuracy for Wave Propagation Problems," *Journal of the Soil Mechanics and Foundations Division*, vol. 99, no. 5, pp. 421–427, May 1973, doi: 10.1061/JSFEAQ.0001885.

[9] M. Mánica, E. Ovando, and E. Botero, "Assessment of damping models in FLAC," *Comput Geotech*, vol. 59, pp. 12–20, Jun. 2014, doi: 10.1016/j.compgeo.2014.02.007.

[10] L. Mejia and E. Dawson, "Earthquake Deconvolution for FLAC," in *Fourth International FLAC Symposium on Numerical Modeling in Geomechanics*, Madrid, Spain, May 2006. [Online]. Available: https://www.researchgate.net/publication/321746982

[11] R. W. Boulanger and K. Ziotopoulou, "PM4Silt (Version 2.1): A silt plasticity model for earthquake engineering applications," Center for Geotechnical Modeling, Department of Civil and Environmental Engineering, University of California, Davis, CA, Report No. UCD/CGM-23/02, Feb. 2023.

[12] E. Naesgaard, "A Hybrid Effective Stress-Total Stress Procedure for Analyzing Soil Embankments Subjected to Potential Liquefaction and Flow," Ph. D. dissertation, The University of British Columbia, Vancouver, BC, Canada, 2011.
[13] J. Macedo, P. Torres, L. Vergaray, S. Paihua, and C. Arnold, "Dynamic effective stress analysis of a centreline tailings dam under subduction earthquakes," *Proceedings of the Institution of Civil Engineers - Geotechnical Engineering*, vol. 175, no. 2, pp. 224–246, Apr. 2022, doi: 10.1680/jgeen.21.00017a.
[14] A. Cerna-Diaz, M. Kafash, R. Davidson, L. Yenne, and P. Doughty, "Nonlinear Deformation Analyses of a Tailings Dam during a Mw5.7 Earthquake," in *Geo-Congress 2023*, Reston, VA: American Society of Civil Engineers, Mar. 2023, pp. 70–85. doi: 10.1061/9780784484708.007.
[15] S. Salam, M. Xiao, A. Khosravifar, and K. Ziotopoulou, "Seismic stability of coal tailings dams with spatially variable and liquefiable coal tailings using pore pressure plasticity models," *Comput Geotech*, vol. 132, p. 104017, Apr. 2021, doi: 10.1016/j.compgeo.2021.104017.
[16] K. M. Rollins, M. Singh, and J. Roy, "Simplified Equations for Shear-Modulus Degradation and Damping of Gravels," *Journal of Geotechnical and Geoenvironmental Engineering*, vol. 146, no. 9, Sep. 2020, doi: 10.1061/(ASCE)GT.1943-5606.0002300.
[17] M. B. Darendeli, "Development of a New Family of Normalized Modulus Reduction and Material Damping Curves," Ph. D. dissertation, University of Texas, TX, USA, 2001.
[18] T. M. Leps, "Review of Shearing Strength of Rockfill," *Journal of the Soil Mechanics and Foundations Division*, vol. 96, no. 4, pp. 1159–1170, Jul. 1970, doi: 10.1061/JSFEAQ.0001433.
[19] N. Barton and B. Kjaersnli, "Shear strength of rockfill," *International Journal of Rock Mechanics and Mining Sciences & Geomechanics Abstracts*, vol. 18, no. 6, p. 111, Dec. 1981, doi: 10.1016/0148-9062(81)90543-X.
[20] H. B. Seed, R. T. Wong, I. M. Idriss, and K. Tokimatsu, "Moduli and Damping Factors for Dynamic Analyses of Cohesionless Soils," *Journal of Geotechnical Engineering*, vol. 112, no. 11, pp. 1016–1032, Nov. 1986, doi: 10.1061/(ASCE)0733-9410(1986)112:11(1016).
[21] J. W. Baker and C. Lee, "An Improved Algorithm for Selecting Ground Motions to Match a Conditional Spectrum," *Journal of Earthquake Engineering*, vol. 22, no. 4, pp. 708–723, Apr. 2018, doi: 10.1080/13632469.2016.1264334.
[22] L. Al Atik and N. Abrahamson, "An Improved Method for Nonstationary Spectral Matching," *Earthquake Spectra*, vol. 26, no. 3, pp. 601–617, Aug. 2010, doi: 10.1193/1.3459159.
[23] E. M. Rathje and J. He, "A Seismic Fragility Framework for Earth Dams," in Lifelines 2022, Reston, VA: *American Society of Civil Engineers*, Nov. 2022, pp. 405–415. doi: 10.1061/9780784484432.036.
[24] J. Macedo, N. Abrahamson, and J. D. Bray, "Arias intensity conditional scaling ground-motion models for subduction zones," *Bulletin of the Seismological Society of America*, vol. 109, no. 4, pp. 1343–1357, Aug. 2019, doi: 10.1785/0120180297.
[25] C. Liu and J. Macedo, "New conditional, scenario-based, and non-conditional cumulative absolute velocity models for subduction tectonic settings," *Earthquake Spectra*, vol. 38, no. 1, pp. 615–647, Feb. 2022, doi: 10.1177/87552930211043897.
[26] C. Liu and J. Macedo, "New conditional, scenario-based, and traditional peak ground velocity models for interface and intraslab subduction zone earthquakes," *Earthquake Spectra*, vol. 38, no. 3, pp. 2109–2134, Aug. 2022, doi: 10.1177/87552930211067817.
[27] J. Macedo, C. Liu, and N. A. Abrahamson, "On the Interpretation of Conditional Ground-Motion Models," *Bulletin of the Seismological Society of America*, vol. 112, no. 5, pp. 2580–2586, Oct. 2022, doi: 10.1785/0120220006.
[28] Federal Emergency Management Agency, "Hazus Earthquake Model Technical Manual – Hazus 5.1," 2022.
[29] J. W. Baker, "Efficient Analytical Fragility Function Fitting Using Dynamic Structural Analysis," *Earthquake Spectra*, vol. 31, no. 1, pp. 579–599, Feb. 2015, doi: 10.1193/021113EQS025M.